

Nonlinear Analysis of Rubber-Based Polymeric Materials with Thermal Relaxation Models

R.V.N. Melnik¹*, D.V. Strunin², A.J. Roberts²

¹ COES, Computational Analysis & Modeling,

Louisiana Tech University, LA 71272, USA

² Department of Mathematics and Computing,

University of Southern Queensland, QLD 4350, Australia

Abstract

Using mathematical modelling and computer simulation, nonlinear dynamics of rubber-based polymers has been studied with due regard for the effect of thermal relaxation. Main results have been obtained for the case of elongational oscillations of a ring-shaped body subjected to periodic (“internal”) boundary conditions. In this case a nonlinear model describing a combined effect of thermal relaxation and thermomechanical coupling has been derived, and the analysis of the behaviour of rubber-based polymers has been conducted numerically. Particular emphasis has been placed on high-frequency and short spatial variations of temperature and displacement where the role of nonlinearities in the dynamics of the material and their close connection with the effect of thermal relaxation time can be best appreciated. It has been shown how the vanishing relaxation time can lead to an attenuation of nonlinear effects in the thermomechanical system.

Key words: hyperbolic thermoelasticity/ nonlinear generalisation of the Lord-Schulman model/ thermomechanical coupling/ rubber-based polymers.

*Corresponding author: Tel.: +1 318 257-3198, Fax: +1 318 257 3823, E-mail: rmelnik@latech.edu

1 Introduction

The effect of thermal relaxation in rubber-based polymers is one of characteristics that render them different from “hard” solids. In idealised solids thermal energy is transported by quantised electronic excitations (free electrons) and by the quanta of lattice vibrations (phonons). A relaxation time appears naturally as the characteristic of thermal resistance in the solid due to dissipative collisions of these quanta. Such thermal resistance is more markedly pronounced in such materials as rubber-based polymers which are important in a wide range of applications [1].

Thermal relaxation is responsible for finite speed of heat propagation. This effect is also known as the “second sound” or the hyperbolic effect due to the type of the equation governing heat propagation [2, 3, 4, 5].

Most contributions to the rigorous analysis of coupled thermomechanical fields in thermoelasticity theory have traditionally been devoted to linear models (see [6] and references therein). Rubber-based polymers provide a classical example where nonlinear effects are essential in the adequate description of the material dynamics. Using the phenomenology of these materials [7, 8], only few recent papers discuss numerical results obtained for these materials with a general nonlinear models of thermoelasticity (see [9, 10, 11, 12] and references therein). Nonlinearities in the dynamics of rubber-based polymers are closely interwoven with the effect of second sound.

So far there have been no attempts to employ the hyperbolic models to study nonlinear thermoelasticity. In order to bridge this gap, our aim in this paper is to explore a combined effect of nonlinearity and thermal relaxation time in rubber-based polymers.

To simplify mathematical analysis we consider elongational oscillations of a ring-shaped body made of the rubber-based polymeric material. An experimental setup for the problem can be thought in the following way. The elastic ring is put inside a circular tube with rigid walls. It is assumed that the tube is lubricated from inside and friction between the polymeric solid material and the tube walls is negligible. When the material is undisturbed, there is no gap between the rubber-based polymer and the walls. Initial local heating will cause a (local) expansion of the rubber-based polymer with its particles having the only freedom to move

along the tube. As a result, one-dimensional thermoelastic waves will start propagating, with volume changes forced by the rigid walls.

This setup gives an example of the dynamics that is attractive from physical point of view and is convenient to study numerically. Indeed, the isolated ring, regarded as a one-dimensional structure, has no boundaries and therefore is not subjected to externally imposed boundary conditions (the periodicity in space can be viewed as an “internal” boundary condition). This property makes the ring an ideal model object for studying intrinsic dynamics of coupled thermomechanical systems. Furthermore, it is important that for systems with such a topology we can effectively employ a relatively simple Fourier-decomposition approach which automatically guarantees the periodicity of the unknown fields.

The paper is organised as follows. In Section 2 we formulate basic balance equations governing the dynamics of the material. In Section 3 we complement them by constitutive relations and in Section 4 we specify the free energy function allowing for the volumetric contributions and coupled thermomechanical effects. Section 5 is devoted to a model of elongational oscillations of a ring-shaped structure. The interactions between nonlinear oscillations of the structure, induced by thermomechanical coupling, and the thermal relaxation time are demonstrated by numerical examples in Section 6.

2 Balance equations

We assume that the motion of the rubber-based polymer material is governed by the kinematic laws

$$\mathbf{y} = \mathbf{x} + \mathbf{u}(\mathbf{x}, t), \quad (2.1)$$

where $\mathbf{x} = (x_1, x_2, x_3)$ is the original and $\mathbf{y} = (y_1, y_2, y_3)$ is the deformed configuration of the body, and $\mathbf{u} = (u_1(\mathbf{x}), u_2(\mathbf{x}), u_3(\mathbf{x}))$ is the displacement vector. The motion at each point of the body can be represented by the deformation gradient

$$\mathbf{F} = \left[\frac{\partial y_i}{\partial x_j} \right]_{i,j=1,2,3} = \mathbf{I} + \frac{\partial \mathbf{u}}{\partial \mathbf{x}}, \quad (2.2)$$

where \mathbf{I} is the second order identity tensor.

According to the polar decomposition theorem, this motion can be split into two components, pure deformation and rigid body rotation

$$\mathbf{F} = \mathbf{Q}\mathbf{U} = \mathbf{V}\mathbf{Q}, \quad (2.3)$$

where \mathbf{Q} is a unique orthogonal matrix (the rigid body rotation), while \mathbf{U} and \mathbf{V} are unique positive definite symmetric matrices which define the right Cauchy-Green stretch tensor (the Cauchy strain tensor) and the left Cauchy-Green stretch tensor (the Finger strain tensor), respectively:

$$\mathbf{C} := \mathbf{U}^2 \equiv \mathbf{F}^T \mathbf{F}, \quad \mathbf{B} := \mathbf{V}^2 \equiv \mathbf{F} \mathbf{F}^T. \quad (2.4)$$

During recent years attempts have been taken to develop Eulerian formulations of thermoelasticity which are exclusively based on the Finger tensor as a strain measure (see, for example, [9]. This approach allows us to compute thermoelastic moduli directly in terms of this tensor. In this paper we use a somewhat more classical approach by dealing with the general nonlinear Green (Green-Lagrange-St.Venant) strain tensor given in the form

$$\mathbf{E} = [\epsilon_{ij}]_{i,j=1,2,3} = \frac{1}{2}(\mathbf{D} + \mathbf{D}^T + \mathbf{D}^T \mathbf{D}), \quad (2.5)$$

where the displacement gradient \mathbf{D} is defined by

$$\mathbf{D} = \nabla \mathbf{u} \equiv \mathbf{F} - \mathbf{I}. \quad (2.6)$$

The linearised form of (2.5) is

$$\mathbf{E} = \frac{1}{2}(\mathbf{F}^T \mathbf{F} - \mathbf{I}) = \frac{1}{2}(\nabla \mathbf{u} + \nabla \mathbf{u}^T). \quad (2.7)$$

In the general case, the evolution of a thermoelastic body can be described by a coupled system consisting of three balance equations, for linear momentum, mass, and energy. In the

Eulerian (spatial) setting, where all physical quantities are regarded as functions of \mathbf{y} and t , this system has the form (see [13], p.18, e.g.)

$$\begin{cases} \rho \dot{\mathbf{v}} = \text{div} \mathbf{T} + \mathbf{F}_1, & \dot{\rho} + \rho \text{div} \mathbf{v} = 0, \\ \rho \dot{e} - \mathbf{T} : \bar{\mathbf{D}}(\mathbf{v}) + \text{div} \mathbf{q} = F_2, \end{cases} \quad (2.8)$$

where ρ is the mass density of the material, e is the internal energy (per unit volume), \mathbf{T} is the Cauchy (true) stress tensor that measures the contact force per unit area in the deformed configuration, \mathbf{v} is the velocity vector, \mathbf{q} is the heat flux, $\mathbf{F}_1 = \rho \mathbf{f}_0$ is the density of the applied volumetric body force \mathbf{f}_0 , and F_2 is the heat density (all measured in the body current configuration). By $\dot{\mathbf{a}}$ we denoted the material time derivative of the quantity \mathbf{a}

$$\dot{\mathbf{a}} = \frac{\partial \mathbf{a}}{\partial t} + \mathbf{v} \cdot \nabla \mathbf{a}. \quad (2.9)$$

As usually, the time derivative on the left of this expression is computed at fixed \mathbf{x} , while the time derivative on the right is computed at fixed \mathbf{y} . In what follows we use the dot notation for both frameworks and the velocity function is always written as $\mathbf{v} = \dot{\mathbf{y}}$. The dyadic operations for “single” and “double-dot” products for Cartesian tensors are defined in the standard way [14]:

$$\mathbf{a} \cdot \mathbf{b} = \sum_{m,n=1}^3 e_m \left[\sum_{i=1}^3 a_{mi} b_{in} \right] e_n^T, \quad \mathbf{a} : \mathbf{b} = |\mathbf{a} \cdot \mathbf{b}|, \quad |c| = \sum_{m=1}^3 c_{mm}. \quad (2.10)$$

Finally, the deformation rate tensor $\bar{\mathbf{D}}(\mathbf{v})$ in (2.8) is defined as the symmetric part of the velocity gradient

$$\bar{\mathbf{D}}(\mathbf{v}) = \text{sym}(\dot{\mathbf{F}} \mathbf{F}^{-1}) = \frac{1}{2}(\nabla \mathbf{v} + \nabla \mathbf{v}^T). \quad (2.11)$$

Note that the last part of this equality is written in the Lagrangian coordinates where we have

$$\dot{\mathbf{F}} = \nabla_{\mathbf{x}} \mathbf{v}. \quad (2.12)$$

Since \mathbf{T} measures force per unit area in the present (deformed) configuration of the body, the use of \mathbf{T} in the Eulerian setting is most natural [15]. In compressible applications of thermoelasticity theory the assumption of isochoric (or volume preserving) deformations, $J \equiv \det \mathbf{F} = 1$, can be violated locally, and hence the system (2.8) is often transformed to another form. Such transformations usually involve the multiplication of balance equations for momentum and energy by J and the use of the Lagrangian form of the balance-of-mass equation [9, 11]. The resulting equations are written then in terms of the weighted Cauchy tensor (the Kirchhoff stress) $\hat{\mathbf{T}} = J\mathbf{T}$.

Under constraints like those described in the Introduction the rubber-based polymers and other complex solid polymers exhibit volume changes [16, 17, 18]. The equivalent Lagrangian (referential) form of problem (2.8) is

$$\begin{cases} \rho_0 \ddot{\mathbf{y}} = \operatorname{div} \boldsymbol{\sigma} + \rho_0 \mathbf{f}_0, & \rho = J^{-1} \rho_0, \\ \rho_0 \dot{e} - \boldsymbol{\sigma}^T : (\nabla \mathbf{v}) + \rho_0 \operatorname{div} \mathbf{q} = F_2, \end{cases} \quad (2.13)$$

where $\boldsymbol{\sigma} = J\hat{\mathbf{F}}^T \mathbf{T}$ is the nominal stress tensor that measures force per unit area in the reference configuration ($\hat{\mathbf{F}} = (\mathbf{F}^T)^{-1}$ (e.g. [8], p. 153), and $\boldsymbol{\sigma}^T = J\mathbf{T}\hat{\mathbf{F}}$ is the first Piola-Kirchhoff stress tensor (see [19], p. 178). Of course, $\boldsymbol{\sigma}$ is generally not symmetric (e.g. Renardy et al., 1987) and the condition $\boldsymbol{\sigma}\mathbf{F}^T = \mathbf{F}\boldsymbol{\sigma}^T$ is equivalent to the symmetry of $\mathbf{T} = J^{-1}\mathbf{F}\boldsymbol{\sigma}$ ([8], p.509). The formulation (2.13) is used as the basis for our computational experiments.

3 Constitutive relations for rubber-based polymeric materials: stress-strain and strain-energy functions

It is well-known that the volume preserving part of the strain energy function can be approximated in terms of the three principal semi-axes of the strain ellipsoid (or simply, extension ratios $\lambda_i, i = 1, 2, 3$ corresponding to principal stresses) by assuming that the initial state (x_0, y_0, z_0) is deformed via the affine deformation

$$x = \lambda_1 x_0, \quad y = \lambda_2 y_0, \quad z = \lambda_3 z_0. \quad (3.1)$$

Mathematically the squares of these extension ratios can be defined as the eigenvalues of \mathbf{C} (or \mathbf{B}) [12]. If we further assume that there is no change of internal energy during deformation, we can define the elastic property of rubber-based polymeric materials in the Gaussian region by the strain-energy relation that follows from the standard thermodynamic analysis (e.g. [7], p. 65)

$$\psi_e(\mathbf{E}) = \theta_0 \Delta S = \frac{1}{2} G \sum_{i=1}^3 (\lambda_i^2 - 1), \quad (3.2)$$

where ΔS is the total entropy of deformation, ψ_e is the elastic part of the free energy function per unit volume of the material, and θ_0 is the absolute temperature. The shear modulus, G , in (3.2) is defined by

$$G = Nk\theta_0 = \rho R\theta_0/M_c, \quad (3.3)$$

where k is the bulk modulus, R is the gas constant per mole, N is the number of chains per unit volume, M_c is the (number average) chain molecular weight. The above expression for the elastic part of the free energy function has been derived under isothermal conditions [7, 12] and strictly speaking can be applied to reversible isothermal processes only. In this case the stress-strain relation is given by

$$\mathbf{S} = 2\rho_0 \frac{\partial \psi_e}{\partial \mathbf{C}} = \rho_0 \frac{\partial \psi_e}{\partial \mathbf{E}}, \quad (3.4)$$

where \mathbf{S} is the second Piola-Kirchhoff stress connected with the Cauchy stress tensor by the standard relationship $\mathbf{S} = J\mathbf{F}^{-1}\mathbf{T}\hat{\mathbf{F}}$ (e.g. [20]) or, equivalently, $T = J^{-1}\mathbf{F}\mathbf{S}\mathbf{F}^T$ [12]. The relation (3.4), exact for the isothermal and isentropic processes, defines hyperelastic (or Green elastic) materials as opposed to Cauchy elastic materials that have a non-conservative structure (e.g. [8], p. 176). The Cauchy stress for hyperelastic materials is given by $\mathbf{T} = \rho \frac{\partial \psi_e}{\partial \mathbf{F}} \mathbf{F}^T$ where the derivative is taken for fixed temperature θ (see [21], p. 266; [12], p. 64). Taking into account that $\mathbf{F} \frac{\partial \psi_e}{\partial \mathbf{E}} = \frac{\partial \psi_e}{\partial \mathbf{F}} = \frac{\partial \psi_e}{\partial \mathbf{E}} \mathbf{F}^T$ we get the expression for the nominal stress

that we use in our computations with the model (2.13) (e.g. [8], p. 153)

$$\boldsymbol{\sigma} = \rho_0 \frac{\partial \psi_e}{\partial \mathbf{E}} \mathbf{F}^T \equiv \rho_0 H(\mathbf{F}), \quad \text{where} \quad H(\mathbf{F}) = \frac{\partial \psi_e}{\partial \mathbf{F}}(\mathbf{F}). \quad (3.5)$$

This gives an interpretation of the nominal stress as the elastic response function $H(\mathbf{F})$ of a material under consideration. Rubber-based polymeric materials provide a prime example where such a response is essentially nonlinear. Due to the nonlinearity, in the general case (3.2) has to be corrected to allow for the non-Gaussian chain statistics. Many authors use the standard Mooney correction of the elastic part of the free energy

$$\psi_e = C_1 \sum_{i=1}^3 (\lambda_i^2 - 1) + C_2 \sum_{i=1}^3 (\lambda_i^{-2} - 1), \quad (3.6)$$

where C_1 and C_2 are given constants. The main disadvantage of this approach is that, using the representation (3.6) (as well as (3.2)) for the elastic part of the free energy function, it is difficult to separate isochoric (deviatoric) and volumetric contributions. An alternative representation of the volume preserving part of the strain energy function ($\psi_e(\mathbf{E})$) is given in terms of the strain invariants of right or left modified Cauchy-Green tensor $\bar{\mathbf{C}} = J^{-2/3} \mathbf{C}$ and $\bar{\mathbf{B}} = J^{-2/3} \mathbf{B}$, respectively

$$\bar{I}_1 = \sum_{i=1}^3 \bar{\lambda}_i^2, \quad \bar{I}_2 = \sum_{i=1}^3 \bar{\lambda}_i^{-2}, \quad (3.7)$$

where $\bar{\lambda}_i = J^{-1/3} \lambda_i$, $i = 1, 2, 3$ are the eigenvalues of $\bar{\mathbf{C}}$ known as the modified principal deviatoric stretches which satisfy the standard incompressibility condition $\prod_{i=1}^3 \bar{\lambda}_i = 1$ [12]. Then the elastic part of the free energy function can be given in the Rivlin form

$$\psi_e = \sum_{i,j=0}^N C_{ij} (\bar{I}_1 - 3)^i (\bar{I}_2 - 3)^j, \quad C_{00} = 0, \quad (3.8)$$

that describes the Mooney-Rivlin materials when $N = 1$ (as well as neo-Hookean materials when, in addition, $C_{01} = 0$). Unfortunately, in the general case the elastic part of the free energy function represented in the form (3.8) cannot be decoupled in the principal directions,

and therefore fails to satisfy the Valanis-Landel hypothesis requiring separability of the strain-energy function

$$\psi_e = \sum_{i=1}^3 w(\bar{\lambda}_i). \quad (3.9)$$

A theoretical justification of this condition is provided by the Taylor expansion of ψ_e near the isochoric pure dilatation $\bar{\lambda}_i = 1$ in $\bar{\lambda}_i - 1$. It can be shown (see [8], p. 494) that up to the 5th order ψ_e can be represented in a separable form. In this paper we use the Ogden form of the strain-energy function which automatically satisfies the Valanis-Landel hypothesis:

$$\psi_e = \sum_{i=1}^3 \sum_{j=1}^N \frac{\mu_j}{\alpha_j} (\bar{\lambda}_i^{\alpha_j} - 1), \quad (3.10)$$

where $N \geq 3$, μ_j , α_j , $j = 1, \dots, N$ are material-dependent constants. We note that the expression (3.10) (and other approximations of the elastic part of the free energy function discussed above) does not allow automatically for thermal effects. However, these effects are critical for rubber-based polymeric materials, and the dependence of constitutive relation on temperature will be a subject of our discussion in the next section.

4 Approximations of the free energy function

There are two important issues to be discussed in this section.

Firstly, for the rubber-based material under constraints, which we consider in this paper, the volumetric contribution is essential. In this case, one of the typical assumptions imposed on the free energy function is its decoupled structure which is usually exploited in the literature in the context of numerical experiments conducted for rubber-like materials [22]. However, it is known now that in the general case the free energy function cannot be split as a pure sum of two components, one is due to shear (elastic part) and the other is due to volume change [12]. Therefore, in the general case a proper inclusion of volumetric contributions into the free energy function is a non-trivial task.

Secondly, as we mentioned before, the stress-strain relation discussed in the previous sec-

tion (see (3.4), (3.5), e.g.) remains, in essence, uncoupled with the temperature field of the material. We emphasise, however, that the thermomechanical coupling is a key phenomena for rubber-based polymeric materials and uncoupled models may lead to misleading results in computing the dynamic behaviour of these materials.

4.1 Allowing for volumetric contributions

Formally, for an arbitrary dilatation parameter $\epsilon = J - 1$ we can take into account the volumetric part of the free energy function by splitting the free energy function into distortional and dilatational components¹

$$\psi_e(\bar{\lambda}_1, \bar{\lambda}_2, J) = \psi_e(\bar{\lambda}_1, \bar{\lambda}_2, 1) + \epsilon \frac{\partial \psi_e}{\partial J} + k_g \tilde{g}(J), \quad (4.1)$$

where \tilde{k}_g is the ground-state bulk modulus in pure dilatation (i.e. where $\bar{\lambda}_1 = \bar{\lambda}_2 = 1$), and $g(J)$ is a function chosen from the consistency conditions with the classical theory (see [8], p. 518). Since the dilatation parameter is typically small in the context of rubber-like polymeric materials most widely used in applications ($\sim 10^{-4}$), this function can often be chosen as identical zero and the decomposition of the motion into a volume preserving distortional part and a dilatational part can be simplified. Indeed, in this case the dilatation effect can be well approximated by the following expansion (typically the first two terms will do the job)

$$\psi_e(\bar{\lambda}_1, \bar{\lambda}_2, J) = \sum_{i=0}^{\infty} \epsilon^i \frac{\partial^i \psi_e}{\partial J^i}(\bar{\lambda}_1, \bar{\lambda}_2, 1). \quad (4.2)$$

Unfortunately, as we mentioned earlier, in the general case the free energy function cannot be represented as a simple sum of its volumetric and isochoric components. Below we explain how the coupling between these two components can be taken into account.

¹Recall that in the decomposition of the strain $\mathbf{E} = \mathbf{E}^* + 1/3(\text{tr}(\mathbf{E}))\mathbf{I}$, \mathbf{E}^* is called the distortional part of the strain and $\text{tr} \mathbf{E}$ is the dilatational part (e.g. [8], p. 348).

4.2 Thermomechanical coupling via the free energy function

We effectively couple volumetric and isochoric parts of the free energy function by introducing a coupling factor $f(\theta)$ [12]

$$\psi(\mathbf{E}, \theta) = \psi_{\text{vol}}(J, \theta) + f(\theta)\psi_{\text{iso}}(\mathbf{E}, \theta), \quad (4.3)$$

where we use a new notation, ψ , for the free energy function (instead of the old one, ψ_e) to reflect its dependency on temperature. The volumetric part of the free energy function, ψ_{vol} , is determined via the penalty arguments

$$\psi_{\text{vol}} = \sum_{i=1}^{\bar{N}} D_i (\theta - 1)^{2i}, \quad \bar{N} \geq 1 \quad (4.4)$$

with D_i being interpreted as penalty for imposing the incompressibility constrain. By setting $\theta = \theta_0$ (which leads to $\psi_{\text{vol}} = 0$) and $f(\theta) = 1$ representation (4.3) is reduced to the classical incompressible case where $\psi_{\text{iso}} = \psi_e \equiv \psi$ is a function of $\bar{\lambda}_i, i = 1, 2, 3$ only. In the general case, however, function ψ_{iso} is dependent on both strain \mathbf{E} and temperature θ and represented as a sum of two parts, equilibrium, ψ_1 , and non-equilibrium, ψ_2 ,

$$\psi_{\text{iso}}(\mathbf{E}, \theta) = \psi_1 + \psi_2. \quad (4.5)$$

Following [11], we postulate the following form of these functions

$$\psi_i = \delta_i \psi_i^0 - \beta_{jk} \epsilon_{jk} (\theta - \theta_0) + e_i^0 \left(1 - \frac{\theta}{\theta_0} \right), \quad i = 1, 2, \quad j, k = 1, 2, 3, \quad (4.6)$$

where e_1^0 is the internal (equilibrium) energy part at the reference temperature θ_0 , ψ_1^0 is the free energy at the temperature θ_0 , ϵ_{jk} are components of the strain tensor \mathbf{E} , and β_{jk} are elements of the thermoelastic pressure matrix (in the linear case, it is the matrix product between the matrix of elastic moduli and the thermal expansion matrix). For functions e_1^0

and ψ_1^0 in (4.6) we choose the following approximations

$$e_1^0 = k_0 \alpha_0 \theta_0 \log J, \quad \psi_1^0 = \sum_{i=1}^3 \frac{\mu_i}{\alpha_i} \sum_{j=1}^3 (\bar{\lambda}_j^{\alpha_i/2} - 1) + \frac{k_0}{4} (J^2 - 2 \log J - 1), \quad (4.7)$$

where k_0 is the bulk modulus, and α_0 is the thermal expansion coefficient. Finally,

$$\delta_1 = \frac{\theta}{\theta_0} + \frac{\partial g}{\partial \theta} \Big|_{\theta=\theta_0} (\theta_0 - \theta) + (g(\theta) - g(\theta_0)), \quad (4.8)$$

where $g(\theta)$ is the shear-moduli-related function determined by fitting experimental data. We define this function as

$$g(\theta) = b \left(\frac{\theta}{\theta_0} \right)^a + d, \quad (4.9)$$

which, by choosing appropriate parameters a , b , and d , allows us to model a wide range of material behaviour, ranging from stiffening to softening [11].

Using arguments of [9] (see also p. 366 in [11]), in our work we set $\psi_2 = 0$. In this case the resulting free energy function is an analogue of the Taylor expansion of the Helmholtz free energy function in the vicinity of the natural state ($\epsilon_{ij} = 0$ and $\theta = \theta_0$) in the classical linear theory of thermoelasticity [23]

$$\psi(\mathbf{E}, \theta) = \psi(0, \theta_0) + \frac{1}{2} c_{ijkl} \epsilon_{ij} \epsilon_{kl} - \beta_{ij} \epsilon_{ij} (\theta - \theta_0) - \frac{\tilde{c}(\theta - \theta_0)^2}{2\theta_0}, \quad (4.10)$$

where \tilde{c} is the heat capacity, c_{ijkl} is the elastic coefficients tensor.

For computational experiments reported in Section 6, the volumetric part of the free energy function in (4.3) is chosen in the form

$$\psi_{\text{vol}} = \bar{c} (\theta - \theta_0 - \theta \log \theta / \theta_0), \quad (4.11)$$

where \bar{c} is the rigid heat capacity [9]. Having the free energy function, the internal energy

(per unit reference volume) is determined via the entropy, η , in the standard manner as

$$e = \psi + \theta\eta, \quad \eta = -\frac{\partial\psi}{\partial\theta}. \quad (4.12)$$

The general form of the free energy function brings appropriate corrections to the stress-strain relation. Recall that since ψ_e is just an isothermal part of the free energy function, the stress-strain relation (3.4) or (3.5) can be “exact” only for isentropic (η is kept constant) or isothermal (θ is kept constant) processes. In the context of entropy elastic materials we have to cover a more general case, hence we refine approximations (3.4), (3.5) as follows

$$\boldsymbol{\sigma} = \boldsymbol{\sigma}(\boldsymbol{\Lambda}, \bar{\mathbf{D}}), \quad \text{and as a special case,} \quad \boldsymbol{\sigma} = \rho_0 \frac{\partial\psi}{\partial\mathbf{F}}, \quad \text{or} \quad \mathbf{S} = \rho_0 \frac{\partial\psi}{\partial\mathbf{E}}, \quad (4.13)$$

where $\boldsymbol{\Lambda}$ is a set of independent variables chosen for the adequate description of material behaviour and such that the entropy inequality is satisfied (see Section 5.3 in [21] for details). The free energy function (per unit reference volume), ψ , in (3.13) is determined by (4.3).

Two final remarks of this section go to viscous and rheological effects. The viscous effects become detectable in the rubber-like polymeric materials when impulse diffuses through the material in the process of microscopic motion of particles. Clearly, these effects can easily be incorporated by including the viscosity tensor into the set $\boldsymbol{\Lambda}$, and, consequently, into the equation of motion and the energy balance equation [24, 21], or by adding to the system (2.13) ((2.8)) an additional equation for the “elastic” part of the Finger strain tensor [11]. We will not pursue these ideas here, and the reader can consult the above cited papers on these standard procedures. Instead, in what follows the main focus will be on the effect of thermal relaxation and its influence on the nonlinear dynamics of the thermomechanical system. This effect is introduced into our model by the Cattaneo-Vernotte (CV) equation

$$\tau_0 \dot{\mathbf{q}} + \mathbf{q} = -\mathcal{K} \nabla \theta, \quad (4.14)$$

where \mathbf{q} is the heat flux, \mathcal{K} is the heat conduction coefficient, and τ_0 is the thermal relaxation time. This equation evolves into the standard Fourier law, $\mathbf{q} = -\mathcal{K} \nabla \theta$, in the limit of vanishing

relaxation time $\tau_0 \rightarrow 0^+$.

Finally, we note that the model described in this section may be enhanced to include rheological effects. This can readily be handled with known procedures (e.g. [11]).

5 Elongational oscillations of a ring-shaped structure

The definition of the strain according to formula (2.2) (and ultimately, the definition of the free energy function) requires the specification of kinematic laws (2.1). As soon as such laws are specified for the rubber-based polymeric material, we can perform the analysis of nonhomogeneous situations where the strains may vary from point to point in the deformed body.

The ring-shaped structure described in the Introduction performs the one-dimensional elongational motion defined by the kinematics

$$y_1 = x_1 + u(x_1, t), \quad y_2 = x_2, \quad y_3 = x_3. \quad (5.1)$$

It must be emphasised that this motion can be exhibited in compressible materials only. The law (5.1) is clearly different from that of the elongational motion under near-incompressibility conditions [15], for example, $y_1 = x_1 + u(x_1, t)$, $y_2 = x_2 / \sqrt{1 + u_x(x_1, t)}$, $y_3 = x_3 / \sqrt{1 + u_x(x_1, t)}$.

For the kinematic law (4.1) the deformation gradient (1.2) is defined by the diagonal matrix $\mathbf{F} = \text{diag}(1 + \partial u / \partial x, 1, 1)$. Hence, the Finger strain tensor has the form $\mathbf{B} = \text{diag}((1 + \partial u / \partial x)^2, 1, 1)$ which provides us with $\lambda_1 = \lambda_2 = 1$, $\lambda_3 = (1 + \partial u / \partial x)^2$. Therefore, J as a function of $\partial u / \partial x$, and modified principal deviatoric stretches can be represented in the form

$$J = 1 + \frac{\partial u}{\partial x}, \quad \bar{\lambda}_{1,2} = J^{-1/3}, \quad \bar{\lambda}_3 = \left(1 + \frac{\partial u}{\partial x}\right)^2 J^{-1/3}. \quad (5.2)$$

As rubber-based polymers may exhibit large deformations, in principle the energy and other functions should be taken in the general forms suitable for both small and large deformations. Since in this section we focus only on the case of small perturbations, these general forms can

be reduced to simpler ones by decomposing them into Taylor series in $\partial u/\partial x$ and $(\theta - \theta_0)$. Indeed, substituting (5.2) into ψ_1^0 in (4.7) and retaining only linear and quadratic terms in the Taylor series we get

$$\psi_1^0 = \frac{1}{2} \sum_{i=1}^3 \mu_i \frac{\partial u}{\partial x} + \frac{1}{8} \left[\sum_{i=1}^3 \mu_i (3\alpha_i - 2) + 4k_0 \right] \left(\frac{\partial u}{\partial x} \right)^2 + \dots \quad (5.3)$$

Under the assumption of Section 3.2 the remaining terms in the free energy function (3.3) turn into zero when $\theta = \theta_0$. Referring to [25], we note that for $u \equiv 0$ there should be no internal stresses ($\sigma \equiv 0$). Hence, due to (3.13), we conclude that in the expansion of ψ_1^0 linear terms should be absent, and therefore $\sum_{i=1}^3 \mu_i = 0$. Further, we note that for the available data for many rubber-like polymers [26, 11] $4k_0$ is typically a dominant term in the square brackets of (5.3). This immediately simplifies the relation (4.4) to

$$\psi_1^0 \approx \frac{k_0}{2} \left(\frac{\partial u}{\partial x} \right)^2. \quad (5.4)$$

Then we take the function $g(\theta)$ from (4.9) in the simplest form corresponding to $a = 0$. In this case (4.9) gives $dg/d\theta = 0$ and consequently (4.8) reads as

$$\delta_1 = \frac{\theta}{\theta_0}. \quad (5.5)$$

Substituting (5.5) and (5.4) into (4.6) for $i = 1$ and replacing β_{jk} by a scalar β we obtain

$$\psi_1 \approx \frac{\theta}{2\theta_0} k_0 \left(\frac{\partial u}{\partial x} \right)^2 - \beta(\theta - \theta_0) \frac{\partial u}{\partial x} + k_0 \alpha_0 \theta_0 \left(1 - \frac{\theta}{\theta_0} \right) \frac{\partial u}{\partial x}. \quad (5.6)$$

In view of (4.5) and $\psi_2 = 0$, the formula (5.6) also represents the function ψ_{iso} . Inserting (5.6) and (4.11) into (4.3) in which we assume for simplicity $f(\theta) = 1$ yields the function ψ :

$$\psi = \bar{c} \left(\theta - \theta_0 - \theta \log \frac{\theta}{\theta_0} \right) + \frac{\theta}{2\theta_0} k_0 \left(\frac{\partial u}{\partial x} \right)^2 - (\beta + k_0 \alpha_0) (\theta - \theta_0) \frac{\partial u}{\partial x}. \quad (5.7)$$

Expression (5.7) can be simplified further by decomposing $\log(\theta/\theta_0)$ into Taylor series in small

value $(\theta - \theta_0)/\theta_0$:

$$\log \frac{\theta}{\theta_0} = \log \left(1 + \frac{\theta - \theta_0}{\theta_0} \right) \approx \frac{\theta - \theta_0}{\theta_0} - \frac{1}{2} \left(\frac{\theta - \theta_0}{\theta_0} \right)^2. \quad (5.8)$$

Substituting (5.8) into (5.7) reduces the latter to the form

$$\psi = -\frac{\bar{c}}{2} \frac{(\theta - \theta_0)^2}{\theta_0} + \frac{\theta}{2\theta_0} k_0 \left(\frac{\partial u}{\partial x} \right)^2 - \gamma(\theta - \theta_0) \frac{\partial u}{\partial x}, \quad (5.9)$$

where

$$\gamma = \beta + k_0 \alpha_0.$$

The stress is readily determined by differentiating (5.9) with respect to $\partial u/\partial x$:

$$\sigma = \rho_0 \frac{\theta}{\theta_0} k_0 \frac{\partial u}{\partial x} - \rho_0 \gamma (\theta - \theta_0). \quad (5.10)$$

The energy e is determined from (4.12) with the help of (5.9):

$$e = -\frac{\bar{c}}{2} \frac{(\theta - \theta_0)^2}{\theta_0} + \frac{\bar{c}}{\theta_0} (\theta - \theta_0) \theta + \gamma \theta_0 \frac{\partial u}{\partial x}, \quad (5.11)$$

from where

$$\dot{e} = -\frac{\bar{c}}{\theta_0} (\theta - \theta_0) \dot{\theta} + \frac{\bar{c}}{\theta_0} \dot{\theta} (2\theta - \theta_0) + \gamma \theta_0 \frac{\partial \dot{u}}{\partial x}. \quad (5.12)$$

We note that the first term in the right-hand side of (5.12) contains the small multiplier $(\theta - \theta_0)/\theta_0$. Disregarding this term we get

$$\dot{e} = \frac{\bar{c}}{\theta_0} (2\theta - \theta_0) \dot{\theta} + \gamma \theta_0 \frac{\partial \dot{u}}{\partial x} \approx \bar{c} \dot{\theta} + \gamma \theta_0 \frac{\partial \dot{u}}{\partial x}. \quad (5.13)$$

Using (5.10) we have

$$\sigma^T : (\nabla \mathbf{v}) = \rho_0 \frac{k_0}{\theta_0} \theta \frac{\partial u}{\partial x} \frac{\partial \dot{u}}{\partial x} - \rho_0 \gamma (\theta - \theta_0) \frac{\partial \dot{u}}{\partial x}. \quad (5.14)$$

Now we are in a position to rewrite the momentum and energy balance equations (2.13) using

(5.10), (5.13) and (5.14). Together with the Cattaneo-Vernotte (CV) equation they have the form

$$\begin{cases} \rho_0 \ddot{u} = \frac{k_0}{\theta_0} \theta \frac{\partial^2 u}{\partial x^2} + \frac{k_0}{\theta_0} \frac{\partial \theta}{\partial x} \frac{\partial u}{\partial x} - \gamma \frac{\partial \theta}{\partial x}, \\ \bar{c} \dot{\theta} = -\frac{\partial q}{\partial x} + \frac{k_0}{\theta_0} \theta \frac{\partial u}{\partial x} \frac{\partial \dot{u}}{\partial x} - \gamma(\theta - \theta_0) \frac{\partial \dot{u}}{\partial x}, \\ \tau_0 \frac{\partial q}{\partial t} + q = -\mathcal{K} \frac{\partial \theta}{\partial x}. \end{cases} \quad (5.15)$$

The heat flux q can be excluded from (5.15) in a straightforward manner by (a) differentiating the CV equation with respect to x that leads to

$$\tau_0 \frac{\partial}{\partial t} \left(\frac{\partial q}{\partial x} \right) + \frac{\partial q}{\partial x} = -\mathcal{K} \frac{\partial^2 \theta}{\partial x^2},$$

and (b) substituting therein the derivative $\partial q / \partial x$ extracted from the energy equation. Doing so we obtain

$$\begin{cases} \rho_0 \ddot{u} = \frac{k_0}{\theta_0} \theta \frac{\partial^2 u}{\partial x^2} + \frac{k_0}{\theta_0} \frac{\partial \theta}{\partial x} \frac{\partial u}{\partial x} - \gamma \frac{\partial \theta}{\partial x}, \\ \tau_0 \bar{c} \ddot{\theta} + \bar{c} \dot{\theta} = \mathcal{K} \frac{\partial^2 \theta}{\partial x^2} + \tau_0 k_0 \left[\left(\frac{\partial \dot{u}}{\partial x} \right)^2 + \frac{\partial u}{\partial x} \frac{\partial \ddot{u}}{\partial x} \right] + k_0 \frac{\partial u}{\partial x} \frac{\partial \dot{u}}{\partial x} \\ - \gamma \tau_0 \theta \frac{\partial \dot{u}}{\partial x} - \gamma \tau_0 \theta \frac{\partial \ddot{u}}{\partial x} - \gamma \theta \frac{\partial \dot{u}}{\partial x}. \end{cases} \quad (5.16)$$

Finally, we substitute the expression for \ddot{u} from the momentum equation (in (5.16)) into the energy equation, replace θ for $\theta_0 + T$ ($T = \theta - \theta_0$) and retain only linear and quadratic terms in T and u :

$$\begin{cases} \rho_0 \ddot{u} = k_0 \frac{\partial^2 u}{\partial x^2} - \gamma \frac{\partial T}{\partial x} + \frac{k_0}{\theta_0} \frac{\partial T}{\partial x} \frac{\partial u}{\partial x} + \frac{k_0}{\theta_0} T \frac{\partial^2 u}{\partial x^2}, \\ \tau_0 \bar{c} \ddot{T} + \bar{c} \dot{T} = \left(\mathcal{K} + \tau_0 \frac{\gamma^2 \theta_0}{\rho_0} \right) \frac{\partial^2 T}{\partial x^2} - \tau_0 \frac{\gamma k_0 \theta_0}{\rho_0} \frac{\partial^3 u}{\partial x^3} \\ - \gamma \theta_0 \frac{\partial \dot{u}}{\partial x} + \tau_0 k_0 \left(\frac{\partial \dot{u}}{\partial x} \right)^2 - \tau_0 \frac{2\gamma k_0}{\rho_0} T \frac{\partial^3 u}{\partial x^3} \\ - \tau_0 \frac{2\gamma k_0}{\rho_0} \frac{\partial T}{\partial x} \frac{\partial^2 u}{\partial x^2} - \tau_0 \frac{2\gamma k_0}{\rho_0} \frac{\partial^2 T}{\partial x^2} \frac{\partial u}{\partial x} + \tau_0 \frac{\gamma^2}{\rho_0} T \frac{\partial^2 T}{\partial x^2} + \tau_0 \frac{k_0^2}{\rho_0} \frac{\partial u}{\partial x} \frac{\partial^3 u}{\partial x^3} \\ + k_0 \frac{\partial \dot{u}}{\partial x} \frac{\partial u}{\partial x} - \tau_0 \gamma \dot{T} \frac{\partial \dot{u}}{\partial x} - \gamma T \frac{\partial \dot{u}}{\partial x}. \end{cases} \quad (5.17)$$

It is easy to see that the linearised version of (5.17) coincides with the linear Lord-Shulman model of hyperbolic thermoelasticity [27]. In this sense, the system (5.17) can be viewed as a generalisation of the classical Lord-Schulman theory to nonlinear hyperbolic thermoelasticity [5]. All quantities of the model (4.18) can be non-dimensionalized using appropriate combinations of the dimensional parameters with independent dimensionalities. We have seven dimensional parameters in the model:

$$\begin{aligned} \rho_0 \text{ (g cm}^{-3}\text{)}, \quad k_0 \text{ (g cm}^{-1} \text{s}^{-2}\text{)}, \quad \theta_0 \text{ (K)}, \quad \mathcal{K} \text{ (g cm s}^{-3} \text{K}^{-1}\text{)}, \\ \gamma \text{ (g cm}^{-1} \text{s}^{-2} \text{K}^{-1}\text{)}, \quad \tau_0 \text{ (s)}, \quad \bar{c} \text{ (g cm}^{-1} \text{s}^{-2} \text{K}^{-1}\text{)}. \end{aligned} \quad (5.18)$$

In (4.19) there are only four parameters with independent dimensionalities, and using $(\rho_0, k_0, \theta_0, \mathcal{K})$ as those, we obtain the following dimensional scales:

$$x_* = \frac{\rho_0^{1/2} \mathcal{K} \theta_0}{k_0^{3/2}}, \quad t_* = \frac{\rho_0 \mathcal{K} \theta_0}{k_0^2}, \quad T_* = \theta_0. \quad (5.19)$$

Omitting algebraic rearrangements, we write the non-dimensional system where, for simplicity, we use the same variables' notations as above:

$$\left\{ \begin{aligned} \ddot{u} &= \frac{\partial^2 u}{\partial x^2} - \frac{C}{B} \frac{\partial T}{\partial x} + \frac{\partial T}{\partial x} \frac{\partial u}{\partial x} + T \frac{\partial^2 u}{\partial x^2}, \\ A\ddot{T} + \dot{T} &= \left(B + \frac{AC^2}{B} \right) \frac{\partial^2 T}{\partial x^2} - AC \frac{\partial^3 u}{\partial x^3} - C \frac{\partial \dot{u}}{\partial x} + AB \left(\frac{\partial \dot{u}}{\partial x} \right)^2 \\ &\quad - 2AC T \frac{\partial^3 u}{\partial x^3} - 2AC \frac{\partial T}{\partial x} \frac{\partial^2 u}{\partial x^2} - 2AC \frac{\partial^2 T}{\partial x^2} \frac{\partial u}{\partial x} + \frac{AC^2}{B} T \frac{\partial^2 T}{\partial x^2} \\ &\quad + AB \frac{\partial u}{\partial x} \frac{\partial^3 u}{\partial x^3} + B \frac{\partial \dot{u}}{\partial x} \frac{\partial u}{\partial x} - AC \dot{T} \frac{\partial \dot{u}}{\partial x} - C T \frac{\partial \dot{u}}{\partial x}, \end{aligned} \right. \quad (5.20)$$

and

$$A = \frac{\tau_0 k_0^2}{\rho_0 \mathcal{K} \theta_0}, \quad B = \frac{k_0}{\theta_0 \bar{c}}, \quad C = \frac{\gamma}{\bar{c}}.$$

In the ring-shaped body of the perimeter L , thermomechanical fields are spatially periodic with the period L linked to the basis wave number $k = 2\pi/L$. We introduce fields of velocity and rate of temperature change, $v = \partial u / \partial t$, $q = \partial T / \partial t$, and seek the solution to (4.21) in

the form of Fourier series

$$\begin{aligned} u &= \sum_{n=-\infty}^{\infty} U_n(t) e^{inkx}, & v &= \sum_{n=-\infty}^{\infty} V_n(t) e^{inkx}, \\ T &= \sum_{n=-\infty}^{\infty} T_n(t) e^{inkx}, & q &= \sum_{n=-\infty}^{\infty} Q_n(t) e^{inkx}. \end{aligned} \quad (5.21)$$

Substituting (5.21) into (5.20) and equating coefficients near $\exp(ink_0x)$ leads to an infinite system of coupled ordinary differential equations for the Fourier-amplitudes:

$$\left\{ \begin{aligned} dU_n/dt &= V_n, \\ dV_n/dt &= -(nk)^2 U_n - \frac{C}{B} ink T_n \\ &\quad - k^2 \sum_{m=-\infty}^{\infty} m(n-m) T_m U_{n-m} - k^2 \sum_{m=-\infty}^{\infty} m^2 U_m T_{n-m} \\ dT_n/dt &= Q_n, \\ AdQ_n/dt &= -Q_n - \left(B + \frac{AC^2}{B} \right) (nk)^2 T_n + ACi(nk)^3 U_n - Cink V_n \\ &\quad - ABk^2 \sum_{m=-\infty}^{\infty} m(n-m) V_m V_{n-m} + 2ACik^3 \sum_{m=-\infty}^{\infty} m^3 U_m T_{n-m} \\ &\quad + 2ACik^3 \sum_{m=-\infty}^{\infty} m(n-m)^2 T_m U_{n-m} + 2ACik^3 \sum_{m=-\infty}^{\infty} m(n-m)^2 U_m T_{n-m} \\ &\quad - \frac{AC^2}{B} k^2 \sum_{m=-\infty}^{\infty} (n-m)^2 T_m T_{n-m} + ABk^4 \sum_{m=-\infty}^{\infty} m(n-m)^3 U_m U_{n-m} \\ &\quad - Bk^2 \sum_{m=-\infty}^{\infty} m(n-m) V_m U_{n-m} - ACik \sum_{m=-\infty}^{\infty} m V_m Q_{n-m} - Cik \sum_{m=-\infty}^{\infty} m V_m T_{n-m}. \end{aligned} \right. \quad (5.22)$$

6 Numerical analysis of a combined effect of thermal relaxation and thermomechanical coupling in nonlinear dynamics

In all numerical experiments reported in this section we use the values of model parameters typical for polyisoprene [26]:

$$\begin{aligned}
 \rho_0 &= 0.913 \text{ g cm}^{-3}, \quad k_0 = 2270 \text{ MPa} = 2.27 \cdot 10^{10} \text{ g cm}^{-1} \text{ s}^{-2}, \quad \theta_0 = 293 \text{ K}, \\
 \mathcal{K} &= 0.134 \text{ W m}^{-1} \text{ K}^{-1} = 1.34 \cdot 10^4 \text{ g cm s}^{-3} \text{ K}^{-1}, \\
 \gamma &= 11.8 \cdot 10^5 \text{ N m}^{-2} \text{ K}^{-1} = 1.18 \cdot 10^7 \text{ g cm}^{-1} \text{ s}^{-2} \text{ K}^{-1}, \\
 \bar{c} &= 1905 \text{ J kg}^{-1} \text{ K}^{-1} \cdot 0.913 \text{ g cm}^{-3} = 1.74 \cdot 10^7 \text{ g cm}^{-1} \text{ s}^{-2} \text{ K}^{-1}.
 \end{aligned} \tag{6.1}$$

Substituting these values into (5.19), we obtain

$$x_* = 1.1 \cdot 10^{-9} \text{ cm}, \quad t_* = 6.9 \cdot 10^{-15} \text{ s}.$$

In studying nonlinear dynamics of rubber-based polymeric materials with due regards to the effect of thermal relaxation, the fact that the time scale turns out to be very small is handy for the analysis of this dynamics. Indeed, note that the thermal relaxation time is also small, typically of the order $10^{-15} - 10^{-12}$ s depending on the material. Since the value of t_* is less then or comparable to typical relaxation times, this will ensure the sensitivity of the model to fast processes where the role of thermal relaxation can not be ignored. The associated small value of x_* will allow us to resolve corresponding short spatial variations of thermal and mechanical fields.

However, care must be taken when dealing with the short spatial scales. Indeed, for the fast and spatially short-scale processes, such as the second sound, the physical system is not in the state of local thermodynamic equilibrium and heat carriers should not obey any universal velocity distribution (e.g, Maxwell distribution). As a consequence, a difficulty arises on how to sensibly define the temperature as it cannot be related to the kinetic energy of heat

carriers averaged over some elementary space volume. At atomic length scales such volume may even contain just one carrier so that the averaging procedure loses sense. Traditionally, the elementary volume is assumed to have comparable extensions in all three dimensions (e.g., [28, 29] and references therein).

We define the temperature in a non-traditional way, which is specifically designed for extremely short quasi-one-dimensional waves like the second sound in elastic rings. The definition is similar to that of originally proposed in [28] (see also [30]) where temperature waves—waves of second sound—were studied. The authors of that paper simulated the behaviour of individual atoms in a three-dimensional lattice exposed to an initial heat pulse applied at lattice end. The results were compared to available experimental data on NaF (e.g., [31]) and satisfactory correlation was revealed at qualitative level (see also a more recent paper [29] and references therein). Note that in these experiments the lattice was supposed to be in thermal equilibrium initially but the equilibrium was destroyed by the propagating heat wave. Under these conditions the kinetic temperature was introduced as the kinetic energy of atoms averaged over cross-sectional lattice plane. Thus, the elementary volume was designed to have microscopic extension (comparable to atomic size) in the direction along the wave propagation but extended over many atomic sizes in the transverse direction. Due to the latter property the elementary volume embraced many atoms; this allowed to use the averaging over them when defining the temperature.

In the similar way we define the temperature as the average kinetic energy of heat carriers over elementary volume with extension of the order x_* in the x direction (along the elastic ring) and of much greater extension in transverse direction (across the ring). Having adopted this temperature definition we view the CV equation as the model that well reproduces (although phenomenologically) main properties of the second sound, namely finite propagation velocity and its wavy character.

The first group of experiments was set to demonstrate the influence of thermal relaxation on nonlinear dynamics of the polymeric body. We excited the ring thermally by introducing the initial temperature shown in Fig. 1. Initial displacements and initial time derivatives of

displacements and temperature are kept zero, so that we have

$$T(x, 0) = R \left(1 + \frac{5}{2} \sin(kx) \right)^4, \quad u(x, 0) \equiv 0, \quad \left(\frac{\partial T}{\partial t} \right)_{t=0} \equiv 0, \quad \left(\frac{\partial u}{\partial t} \right)_{t=0} \equiv 0. \quad (6.2)$$

The factor R in (6.2) is chosen so that the temperature at the maximum of the peak is equal to the melting temperature T_m of the polymeric material. For polyisoprene $T_m = 35$ C, consequently the corresponding non-dimensional temperature equals 0.05 which is provided by $R = 10^{-3}/3$. Strictly speaking, once the initial conditions are specified, we are left with the only free parameter in our model, namely the wave number k . However, since the relaxation time is a parameter that is difficult to measure in practice and for most applications its value can be given within a specified range only, it is very instructive to conduct an experiment where the influence of variations in this parameter on the nonlinear dynamics can be investigated. In what follows, we assume that the typical value of τ_0 for the materials under consideration is of the order $\tau_0 \sim 10^{-12}$ s.

We truncate the system (5.22) to a finite number of modes and integrate it in time using the fourth order Runge-Kutta method. In our experiments we used typically 10 Fourier modes which was sufficient to provide an accurate representation of the solution. Due to negligibly small contributions of higher modes to the solution of the problem, we observed practically the same profiles of computed thermomechanical fields when larger numbers of modes were used (up to 30).

In Fig. 2 the dynamics of elongational oscillations is shown for $k = 1$ and $\tau_0 = 10^{-12}$ s. For convenience, all figures display two periods of temperature and displacement profiles (figures (a) and (c)). Next to each 3-D plot we place the last recorded profile (b) and (d), respectively). Thus, the initial profile (Fig. 1) and the profile computed at the last moment of time, t_1 , are presented separately, while intermediate-time profiles can be judged upon the presented 3-D plots. The dynamics considered in this example is very irregular. Indeed, our computations beyond the chosen limiting moment t_1 showed that, eventually, nonlinear effects started to drive the profiles towards the formation of shock-type waves. The moment of the shock wave formation manifests itself by a typical rippling of displacement and temperature profiles, and therefore, can be estimated computationally. In all our experiments we chose the limiting

time t_1 small enough to avoid this phenomenon. The shock wave formation in nonlinear thermoelasticity is a well-known phenomenon (especially in the context of classical models) which has been studied theoretically by a number of researchers (see, for example, [32]).

For smaller values of k representing a “stretched-out” initial temperature peak, a longer period is needed for the nonlinear terms to produce a noticeable effect. For example, Fig. 3 ($k = 0.01$) shows the profiles (of temperature [Fig. 3a] and of displacements [Fig. 3b]) formed by the moment $t_1 = 500$ when the peak changed substantially in height as compared to the initial profile. We found that even after such a relatively long evolution, the nonlinearities still have a negligible effect. This was confirmed by comparing the presented profiles with the profiles obtained with the linearised system (4.21). Another important observation that follows from Fig. 3 is that the profiles corresponding to the relaxation times smaller than 10^{-12} s practically coincide with each other. This is not surprising because, for sufficiently small values of τ_0 , the terms with the relaxation time (see (5.20)) practically vanish. We observe that the profile for a relatively large relaxation time corresponding to $\tau_0 = 10^{-11}$ s is clearly different from the other profiles, while the profile for $\tau_0 = 10^{-12}$ s is just slightly different from the profiles corresponding to smaller values of τ_0 . Therefore, for given wave number $k = 0.01$ the relaxation time $\tau_0 = 10^{-12}$ s can be viewed as “critical” in a sense that one may expect an increasing influence of the effect of thermal relaxation for polymeric materials with larger values of τ_0 . For larger wave numbers k , the nonlinear terms in the energy balance equation play a significant role at earlier stages of the dynamics. Fig. 4 shows profiles of the thermal (Fig. 4a) and mechanical (Fig. 4b) fields for $k = 1$ at the moment $t_1 = 100$. Two curves presented in this figure demonstrate distinctive difference between the results of computations with the full and linearised system (4.21).

In the second group of experiments we investigated a combined effect of thermal relaxation and nonlinear oscillatory dynamics of the thermomechanical body. The main result is illustrated by Fig. 5 ($k = 5$). First, note that the majority of the nonlinear terms in our system (5.20) contain the relaxation time parameter A . By switching from the case $\tau_0 = 10^{-12}$ s to the case $\tau_0 = 10^{-15}$ s we decrease the value τ_0 and, consequently, suppress the nonlinearities. The first term in the right hand side of the energy balance equation (see (4.21)) becomes dominant,

and we observe a damping of temperature, which eventually leads to its almost uniform spatial distribution (Fig. 5b). Thereafter, displacements continue to oscillate obeying, in essence, the usual wave equation of motion.

This phenomenon should be viewed not only as a result of different roles of nonlinearities in the system, but as a combined effect of nonlinearities and thermal relaxation. Although we only demonstrated the significance of this effect for short spatial and temporal scales, it can be foreseen that the role of thermal relaxation can be far from negligible for larger scales. Indeed, the term containing the relaxation time, AC^2/B , makes a substantial contribution to the effective coefficient of temperature dissipation, $(B + AC^2/B)$. For the data (5.1) it can be easily found that $AC^2/B = 0.0026$ and $B = 0.00076$. Although this estimate is pretty rough, it clearly points out to the possibility for the ratio AC^2/B to become appreciable compared to the value of B , even though the value of τ_0 remains small.

7 Conclusions

Using computer simulation we studied thermomechanical behaviour of rubber-based polymeric material with special attention given to the role of the thermal relaxation phenomenon in nonlinear dynamics. We considered elongational oscillations of a ring-shaped body that provided us with an instructive example for studying important features of a combined effect of thermal relaxation and thermomechanical coupling. We derived a nonlinear thermomechanical model based on conventional forms of free energy functions for these polymeric materials and the Cattaneo-Vernotte equation allowing for the effect of thermal relaxation. The model comprising of the equations of motion and energy balance represents a generalisation of the classical Lord-Schulman model, and in the linear case both models are identical. A distinctive feature of our model is its ability to allow for a combined effect of thermal relaxation and nonlinear character of oscillatory dynamics of the thermomechanical system. This effect is most pronounced for high time frequency and short spatial variations of temperature and displacements. This case was analysed numerically with a computational scheme based on the Fourier decomposition of thermomechanical fields. Since most of nonlinear terms in our model contain the thermal relaxation time parameter, we conducted a series of numerical experiments

to reveal a close connection between nonlinear dynamics of the system and the phenomenon of thermal relaxation. In particular, we demonstrated that the vanishing relaxation time can lead to a remarkable damping of nonlinear effects in the dynamics of the thermomechanical system.

8 Acknowledgements

This research was supported by the Australian Research Council Grant 179406.

References

- [1] G. Rabilloud, *High performance polymers: chemistry and applications*, Editions Technip, Paris, 1999.
- [2] D. S. Chandrasekharaiah, Hyperbolic thermoelasticity: A review of recent literature, *Appl. Mech. Rev.*, vol. 51, pp. 705–729, 1998.
- [3] R. B. Hetnarski and J. Ignaczak, Soliton-Like Waves in a Low-Temperature Nonlinear Thermoeleastic Solid, *Int. J. Engng. Sci.*, vol. 34, pp. 1767–1787, 1996.
- [4] K. Saxton, R. Saxton, and W. Kosinski, On Second Sound at the Critical Temperature, *Quart. Appl. Math.*, vol. LVII, pp. 723–740, 1999.
- [5] D. V. Strunin, R.V.N. Melnik, A.J. Roberts, Coupled thermomechanical waves in hyperbolic thermoelasticity, *Journal of Thermal Stresses*, vol. 24 (2), pp. 121–140, 2001.
- [6] R.V.N. Melnik, Discrete models of coupled dynamic thermoelasticity for stress-temperature formulations, *Appl. Math. Comp.*, vol. 122 (1), pp. 107–132, 2001.
- [7] L. R. G. Treloar, *The Physics of Rubber Elasticity*, Clarendon Press, Oxford, 1975.
- [8] R. W. Ogden, *Non-linear elastic deformations*, Wiley & Sons, New York, 1984.
- [9] C. Miehe, Entropic thermoelasticity at finite strains. Aspects of the formulation and numerical implementation, *Comput. Methods Appl. Mech. Engrg.*, vol. 120, pp. 243–269, 1995.
- [10] G.A. Holzapfel and J.C. Simo, Entropy elasticity of isotropic rubber-like solids at finite strains, *Comput. Methods Appl. Mech. Engrg.*, vol. 132, pp. 17–44, 1996.

- [11] S. Reese and S. Govindjee, Theoretical and numerical aspects in the thermo-viscoelastic material behaviour of rubber-like polymers, *Mechanics of Time-Dependent Materials*, vol. 1, pp. 357–396, 1998.
- [12] K.-D. Papoulia, Mixed and selective integration procedures in large strain hyperelastic analysis of nearly incompressible solids, *Computational Mechanics*, vol. 23, pp. 63–74, 1999.
- [13] P. Le Tallec, *Numerical Analysis of Viscoelastic Problems*, Masson, Paris, 1990.
- [14] P. M. Morse and H. Feshbach, *Methods of theoretical physics*, McGraw-Hill, New York, 1953.
- [15] M. Renardy, W.J. Hrusa, and J. A. Nohel, *Mathematical Problems in Viscoelasticity*, Longman, New York, 1987.
- [16] R. Schirrer, C. Fond, and A. Lobbrecht, Volume change and light scattering during mechanical damage in polymethylmethacrylate toughened with core-shell rubber particles, *Journal of Materials Science*, vol. 31, pp. 6409–6422, 1996.
- [17] Y. Yokoyama and T. Ricco, Toughening of polypropylene by different elastomeric systems, *Polymer*, vol. 39, pp. 3675–3681, 1998.
- [18] Y.C. Gao and T. Gao, Mechanical behaviour of two kinds of rubber materials, *Int. J. Solids Structures*, vol. 36, pp. 5545–5558, 1999.
- [19] M.E. Gurtin, *An Introduction to Continuum Mechanics*, Academic Press, New York, 1981.
- [20] S. R. Bodner and M.B. Rubin, A unified elastic-viscoplastic theory with large deformations, In: Gittus, J., Zarka, J., and Nemat-Nasser, S. (Eds.), *Large Deformations of Solids: Physical Basis and Mathematical Modelling*, Elsevier Applied Science, London, pp. 129–140, 1996.
- [21] J. C. Slattery, *Advanced Transport Phenomena*, Cambridge University Press, 1999.
- [22] G.A. Holzapfel, Physical modeling and finite element analysis in rubber thermoelasticity. *ZAMM: Z. Angew. Math. Mech.*, vol. 78(S1), pp. S133–S136, 1998.
- [23] W. Nowacki, *Dynamic problems of thermoelasticity*, Noordhoff IP, Leyden, The Netherlands, 1975.
- [24] D. Potter, *Computational Physics*, Wiley & Sons, London, 1973.

- [25] L. D. Landau and E.M. Lifshitz, *Theory of elasticity*, Butterworth-Heinemann, Oxford/Boston, 1995.
- [26] J. Brandrup, E.H. Immergut, and E. A. Grulke (eds.), *Polymer Handbook*, John Wiley & Sons, N.Y., 1999.
- [27] H.W. Lord and Y. Schulman, A generalized dynamic theory of thermoelasticity, *J. Mech. Phys. Solids*, vol. 15, pp. 299–309, 1967.
- [28] D.H. Tsai and R.A. MacDonald, Molecular-dynamical study of second sound in a solid excited by a strong heat pulse, *Physical Review B*, vol. 14, pp. 4714–4723, 1976.
- [29] J.R. Ho et al, Lattice Boltzmann scheme for hyperbolic heat conduction equation, *Numer. Heat Transfer, Part B*, vol. 41, pp. 591–607, 2002.
- [30] D.D. Joseph and L. Preziosi, Heat waves, *Reviews of Modern Physics*, vol. 61, pp. 41–73, 1989.
- [31] T.F. McNelly et al, Heat pulses in NaF: Onset of second sound, *Physical Review Letters*, vol. 24, pp. 100–102, 1970.
- [32] R. Racke, Blow-up in non-linear three-dimensional thermoelasticity, *Math. Methods Appl. Sci.*, vol. 12, pp. 267–273, 1990.

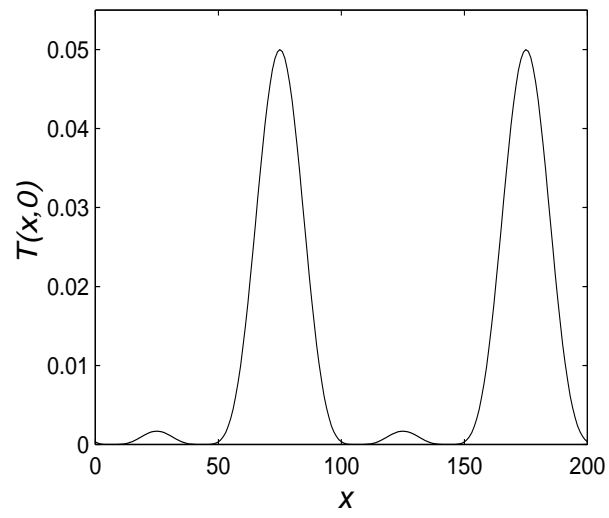


Figure 1:

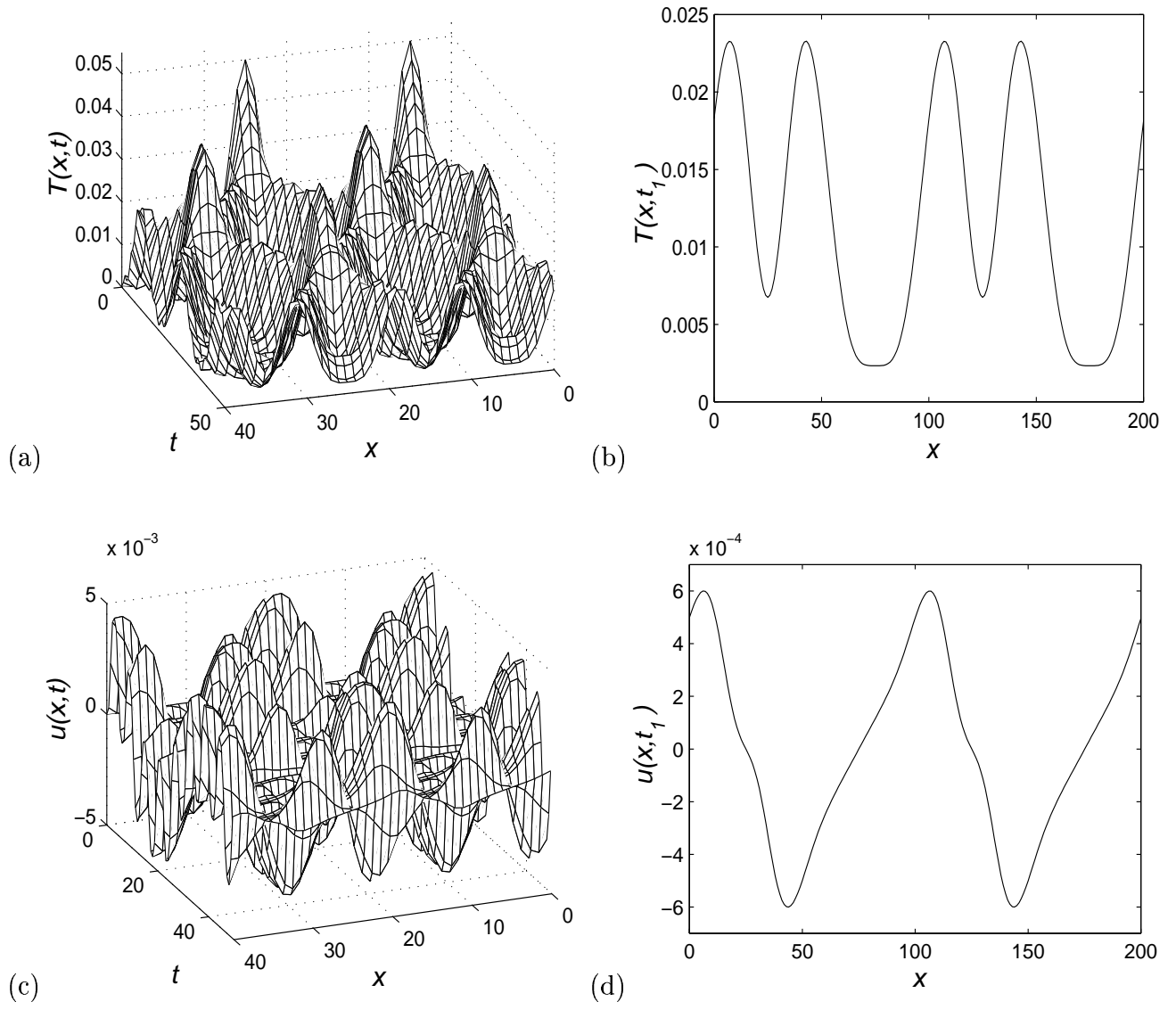


Figure 2:

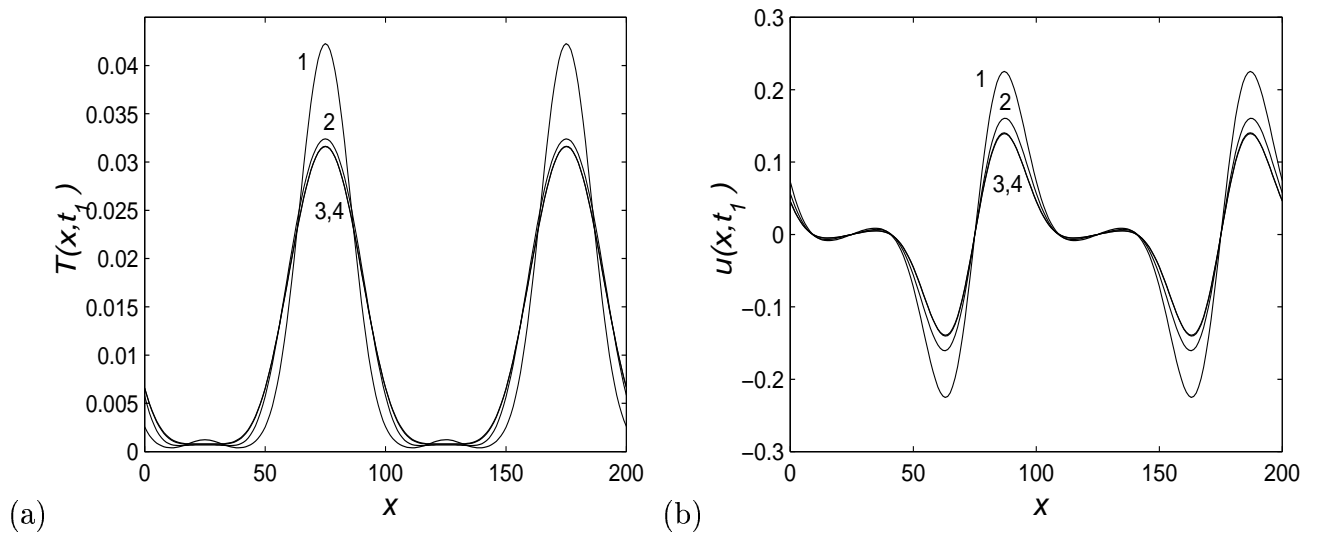


Figure 3:

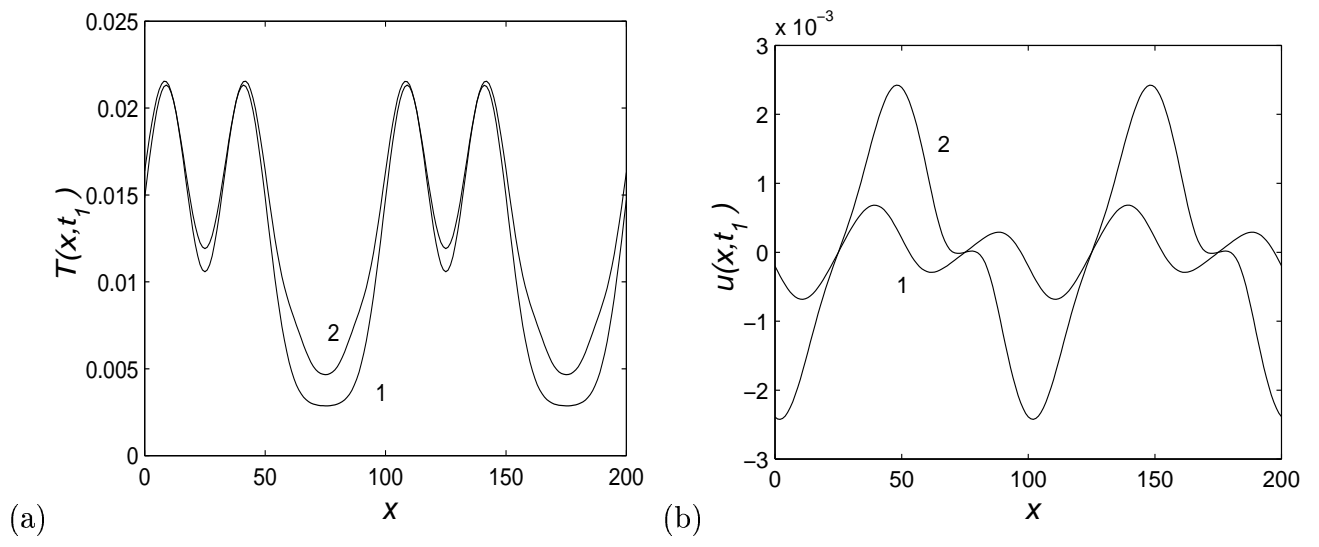


Figure 4:

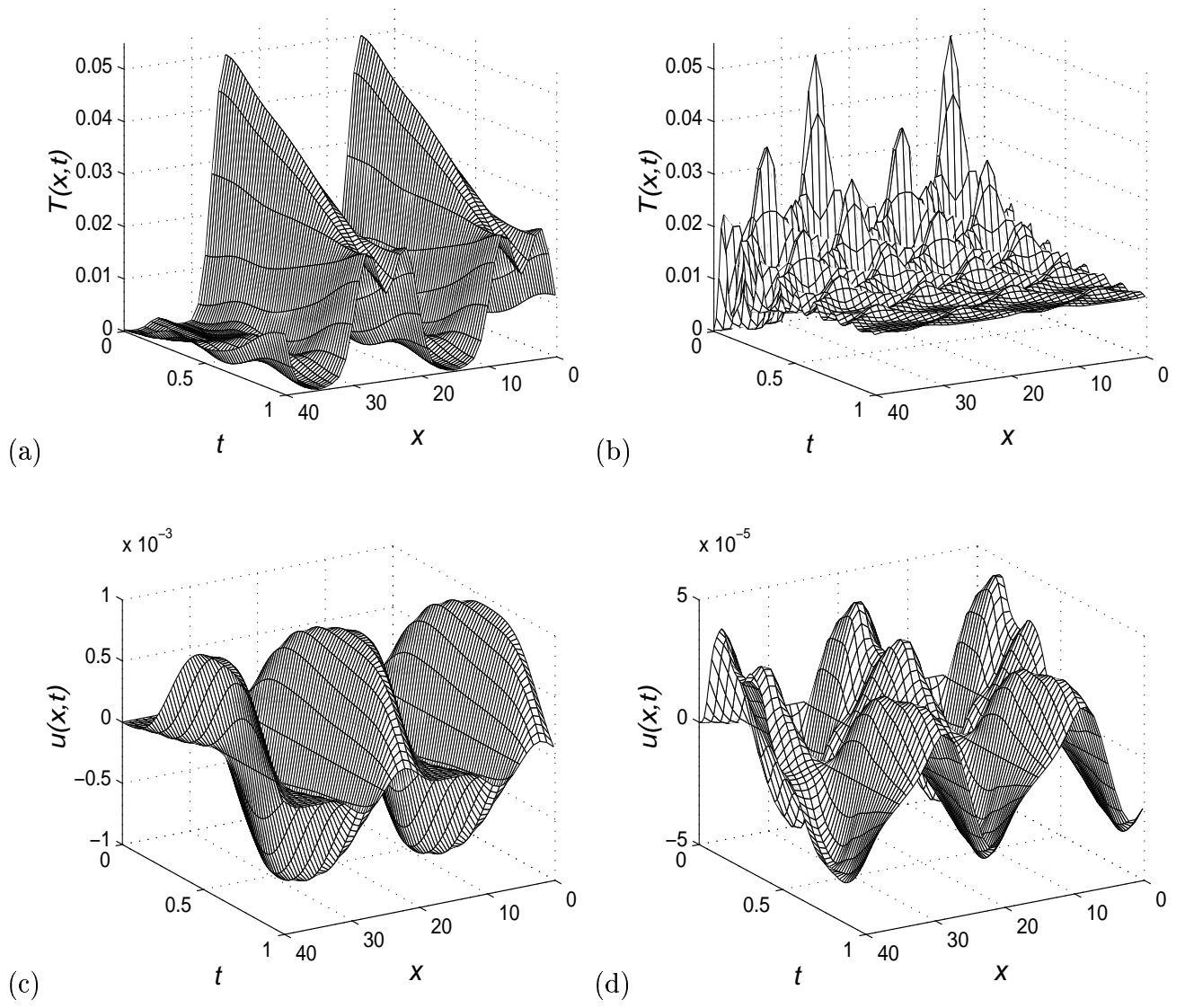


Figure 5:

List of figure captions

- Figure 1: Initial temperature has the form of a peak.
- Figure 2: The dynamics of temperature and displacement ($t_1 = 50$).
- Figure 3: Temperature and displacement for different relaxation times. $\tau_0 = 10^{-11}$ s (1), 10^{-12} s (2), 10^{-13} s (3), 10^{-14} s (4).
- Figure 4: Temperature and displacement obtained with the linear (1) and nonlinear (2) system. $\tau_0 = 10^{-12}$ s.
- Figure 5: Dynamics of temperature and displacement for $\tau_0 = 10^{-12}$ s (left column) and $\tau_0 = 10^{-15}$ s (right column).

List of notation

Latin small characters

- c_{ijkl} is the elastic coefficients tensor;
- \tilde{c} is the heat capacity;
- e is the internal energy (per unit volume);
- e_1^0 is the internal (equilibrium) energy part at the reference temperature;
- \mathbf{f}_0 is the applied volumetric body force;
- $g(J)$ is a given function;
- $g(\theta)$ is the shear-moduli-related function;
- k is the bulk modulus;
- \tilde{k}_g is the ground-state bulk modulus in pure dilatation;
- \mathbf{q} is the heat flux;
- \mathbf{u} is the displacement vector.
- \mathbf{v} is the velocity vector;
- \mathbf{x} is the original (undeformed) configuration of the body;
- \mathbf{y} is the deformed configuration of the body;

Latin capital characters

- \mathbf{B} is the Finger strain tensor;
- \mathbf{C} is the Cauchy strain tensor;
- \mathbf{D} is the displacement gradient;
- D_i is a penalty for imposing the incompressibility constrain;
- \mathbf{F}_1 is the density of the applied volumetric body force;
- F_2 is the heat density;

- G is the shear modulus;
- \mathbf{I} is the second order identity tensor;
- \mathcal{K} is the heat conduction coefficient;
- N is a constant;
- M_c is the (number average) chain molecular weight;
- \mathbf{Q} is the rigid body rotation (an orthogonal matrix);
- R is the gas constant per mole;
- \mathbf{S} is the second Piola-Kirchhoff stress;
- \mathbf{T} is the Cauchy (true) stress tensor;
- \mathbf{U} is a positive definite symmetric matrix;
- \mathbf{V} is a positive definite symmetric matrix;

Greek small characters

- α_0 is the thermal expansion coefficient;
- α_j are material-dependent constants;
- β_{jk} are elements of the thermoelastic pressure matrix;
- ϵ_{jk} are components of the strain tensor;
- θ_0 is the absolute temperature;
- μ_j are material-dependent constants;
- ρ is the mass density of the material;
- $\boldsymbol{\sigma}$ is the nominal stress tensor that measures force per unit area in the reference configuration;
- $\boldsymbol{\sigma}^T$ is the first Piola-Kirchhoff stress tensor;
- τ_0 is the thermal relaxation time;
- ψ is the free energy function;

- ψ_e is the elastic part of the free energy function;
- ψ_{vol} is the volumetric part of the free energy function;
- ψ_1^0 is the free energy at the temperature θ_0 ;

Greek capital characters

- ΔS is the total entropy of deformation;
- Λ is a set of independent variables.